






## A Model for Extracting the Velocity Features of Fluid Movement in Flotation Cells of the Shahr-e Babak Copper Complex Using the PIV Method

M. Eghbali Fard<sup>1</sup>, M. H. Gholizadeh<sup>2</sup> , H. Ghiyoumi Zadeh<sup>2\*</sup> , H. Fatehi Marj<sup>2</sup> 

<sup>1</sup> MSc Student, Department of Electrical Engineering, Vali-e-Asr University of Rafsanjan, Rafsanjan, Iran

<sup>2</sup> Assistant Professor, Department of Electrical Engineering, Vali-e-Asr University of Rafsanjan, Rafsanjan, Iran

<sup>3</sup> Assistant Professor, Department of Electrical Engineering, Vali-e-Asr University of Rafsanjan, Rafsanjan, Iran

<sup>4</sup> Assistant Professor, Department of Electrical Engineering, Vali-e-Asr University of Rafsanjan, Rafsanjan, Iran

ARTICLE INFO	ABSTRACT
<p>Article History:            Received 6 April 2018            Received in revised form 12 June 2018            Accepted 25 September 2018            Available online 2 December 2018</p>	<p>In this study, the flotation process is examined as a conventional method for processing low-grade copper sulfide ores. The performance of this process is influenced by various factors, including the type and dosage of collector, frother, pH regulator, activator, and depressant. Identifying effective reagents and determining optimal conditions are crucial for enhancing efficiency, and modeling and simulation of this process can further aid in its improvement. Traditionally, experienced operators assess and control the process based on the visual characteristics of the froth. However, with advancements in technology, machine vision has emerged as a valuable tool for monitoring and controlling flotation circuits. In this context, a machine vision system was installed on a flotation cell in the rougher circuit of the Shahr-e Babak Copper Flotation Plant to monitor the process under various conditions. The primary visual feature extracted from the captured images is the bubble velocity on the froth surface, which directly impacts flotation performance. In this research, the Particle Image Velocimetry (PIV) technique was employed to determine bubble velocities without the need for additional particles or lasers. Simulation results demonstrate that the proposed method exhibits high accuracy in providing relevant velocity features, making it a potent tool for monitoring and optimizing the performance of flotation cells.</p>
<p>Keywords:            Flotation, Shahr-e Babak, Image Processing, PIV</p>	

### 1. INTRODUCTION

Flotation is a physico-chemical separation process that exploits differences in the surface properties of valuable minerals and unwanted gangue minerals. Flotation cells typically have a cylindrical shape, with their height being significantly greater than their diameter [1-5]. Feed is introduced into the upper half of the cell, and compressed air is injected into the cell from the bottom through spargers. As materials fall under their own weight in the aqueous environment, they collide with rising air bubbles. If they are sufficiently hydrophobic, the particles attach to the

\* Corresponding Author: [h.ghayoumizadeh@vru.ac.ir](mailto:h.ghayoumizadeh@vru.ac.ir)

Assistant Professor, Department of Electrical Engineering, Vali-e-Asr University of Rafsanjan, Rafsanjan, Iran



bubbles and float to the surface, overflowing from the top edge of the column [6]. Copper sulfide ores (with pyrite as the dominant mineral) are among the most important sources of copper, and flotation is commonly used for their processing. This process achieves separation of valuable minerals from gangue minerals in an aqueous environment by altering the physico-chemical properties of the solid surfaces [7]. Modeling and simulating the flotation process is challenging due to the numerous variables and interactions involved. The efficiency of copper sulfide flotation operations in concentrator plants is generally high and acceptable, except when the percentage of clayey and pyritic gangue minerals in the feed increases. Various chemicals such as collectors, depressants, frothers, activators, and regulators are used to achieve optimal recovery and efficiency in the process [8]. Flotation circuits are subject to a wide range of process disturbances, some of which are due to variations in mineral characteristics and other changes in operating conditions.

In most flotation plants, process operators visually monitor the froth surface and make adjustments. In other words, they assess the froth surface based on visual characteristics and adjust production strategies accordingly. However, due to the inherent complexity of the flotation process, achieving optimal control is often not feasible for human operators [9]. Important factors for operators in assessing the froth surface include liquid flow rate, bubble size, and color [10].

Various devices are used to monitor and control flotation circuits. Several efforts have been made to develop effective algorithms for measuring the visual properties of froth. It has been widely reported that bubble size on the froth surface is strongly correlated with operational conditions and process performance [11]. Different techniques for measuring bubble size have been proposed, such as separation, texture spectrum, and the use of interfacial morphological information [12]. Other studies have focused on detecting white spots on the bubble surface, where the size of the white spots corresponds to bubble size and their number inversely correlates with bubble size in the froth image. Proper lighting of the froth surface is crucial in this method [13]. Each of these methods has its own advantages and disadvantages.

In the proposed model, bubble displacement velocity on the froth surface is measured. Common methods for measuring fluid motion parameters include the use of velocimetry equipment for direct measurement of fluid motion. These devices typically measure point-wise and require significant time and expense. In the past two decades, with advances in optical equipment and the use of image processing, indirect methods based on image processing have been introduced for measuring fluid velocity fields and flow rates. These methods obtain fluid motion parameters by imaging fluid motion and analyzing and processing these images. Optical methods for measuring fluid velocity, such as Shadowgraphy, Schlieren, Moiré, interferometry, and optical tomography, have been well-known and utilized since previous decades [14].

In this study, the velocity of fluid motion is practically measured in the flotation cells of the Shahrehabak Copper Complex in Iran using the PIV (Particle Image Velocimetry) method with a new technique that does not use lasers. In the PIV method, particles are added to the fluid, and the fluid velocity, which corresponds to the particle velocity, is calculated using laser illumination. The selection of the type and size of particles used is crucial. Firstly, the chosen particle should have a density close to that of the fluid to prevent settling during the experiment and should follow fluid motion, essentially acting like a fluid element. Additionally, the concentration and diameter of these particles in the fluid should be such that they do not alter the fluid properties. If the particle diameter is large, it provides better light intensity, but if it is too large, the particle will not follow the fluid motion, resulting in inaccurate information. Instead of using particles, in the proposed model, bubbles are separated using image processing techniques, and then the PIV technique is used to calculate particle displacement velocity. In other words, the bubbles on the froth surface play the role of particles in the PIV method.

## **2. MATERIALS AND METHODS**

Optical methods have become highly common in fluid mechanics and have made significant advancements in recent years. One of the most widely used methods in fluid mechanics is the Particle Image Velocimetry (PIV) method [15]. In this method, particles are initially added to the fluid, which follow the fluid properties such as density. Next, these particles are tracked using laser illumination. Images of these particles are then captured, and the film is converted into its constituent frames. By analyzing these frames, fluid velocity vectors are obtained [13]. However, in the innovative method, bubbles themselves are used as particles in the PIV method. The flotation

velocity can be determined by measuring the movement of bubble centers in successive frames. The flowchart of the proposed algorithm is shown in Figure 1.

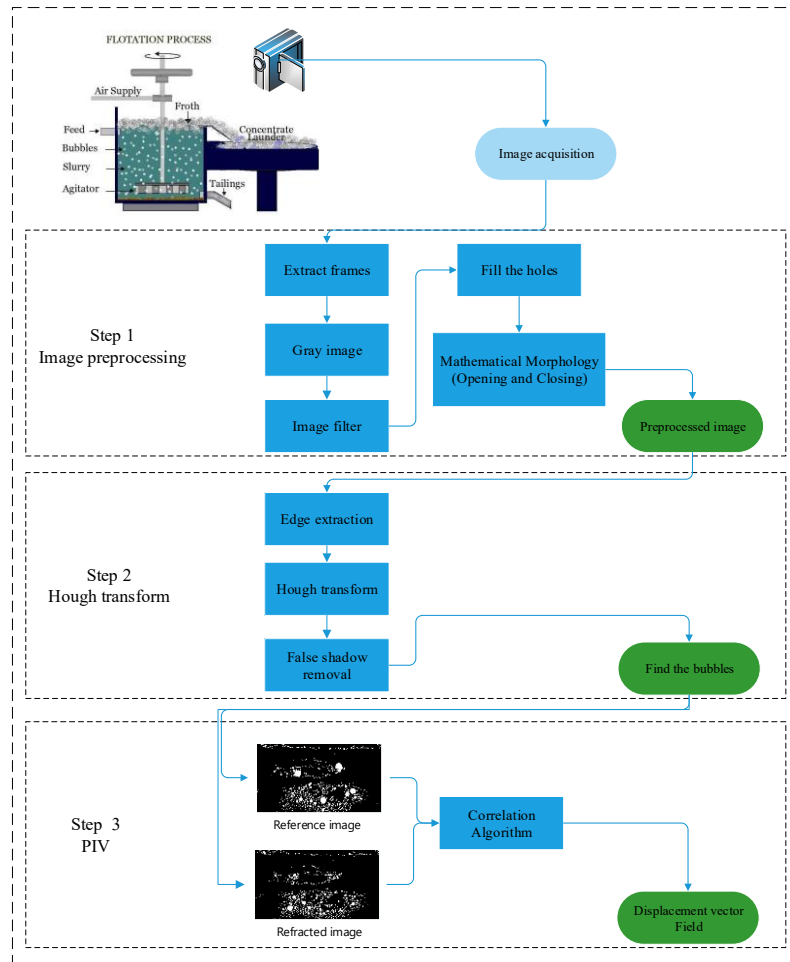


Fig. 1. Block Diagram of Flotation Velocity Estimation Steps

In the first step, pre-processing operations are applied to the image to enhance the quality. A camera is installed on the scavengers, and daily photos and videos are captured to obtain necessary information about fluid movement. A sample image taken from flotation is shown in Figure 2.

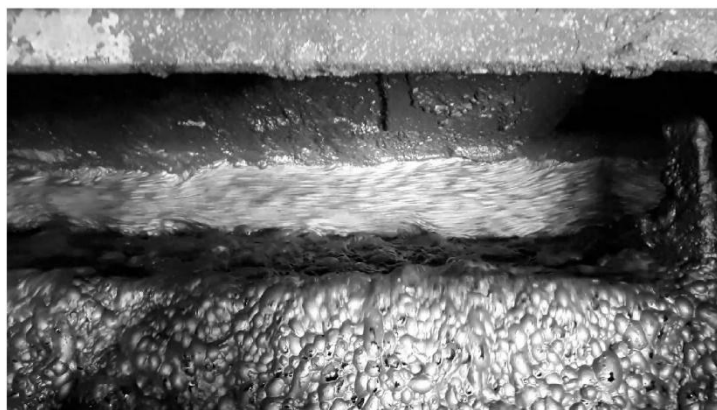


Fig. 2. A Frame from the Flotation Video in Motion

The images extracted from video frames are converted to grayscale images. Then, filters such as averaging filters are applied to reduce image noise. An averaging filter considers a neighborhood around a pixel and takes the average intensity of the pixels within that neighborhood as the new value for that pixel. Typically, the neighborhood around a pixel is considered square, with each side having  $2k+1$  pixels. If the initial image  $I$  has a pixel intensity of  $I(x,y)$  at position  $(x,y)$ , then an averaging filter with a  $(2k+1) \times (2k+1)$  neighborhood changes the pixel intensity from  $I(x,y)$  to  $J(x,y)$  as follows:

$$J(x,y) = \sum_{i=-k}^k \sum_{j=-k}^k \frac{1}{(2k+1)^2} I(x+i,y+j) \quad (1)$$

As can be seen, the averaging filter is a linear filter, and its mask matrix is a  $(2k+1) \times (2k+1)$  matrix with all elements being:

$$w_{i,j} = \frac{1}{(2k+1)^2} \quad (2)$$

Holes in the image are filled using the averaging method.

Next, morphological operations of opening and closing are applied to the image. Opening typically smooths the content of an object, breaks narrow paths, and removes thin protrusions. Closing also smooths parts of the contour but, unlike opening, it joins narrow breaks and long thin gaps, removes small holes, and fills contour spaces in the background. Opening a set  $A$  with a structuring element  $B$  is defined by:

$$A \circ B = (A \ominus B) \oplus B \quad (3)$$

Where  $\ominus$  denotes erosion and  $\oplus$  denotes dilation. Similarly, closing a set  $A$  with a structuring element  $B$  is defined by:

$$A \bullet B = (A \oplus B) \ominus B \quad (4)$$

Two samples of sequential frames extracted from the video images are shown in Figure 3.

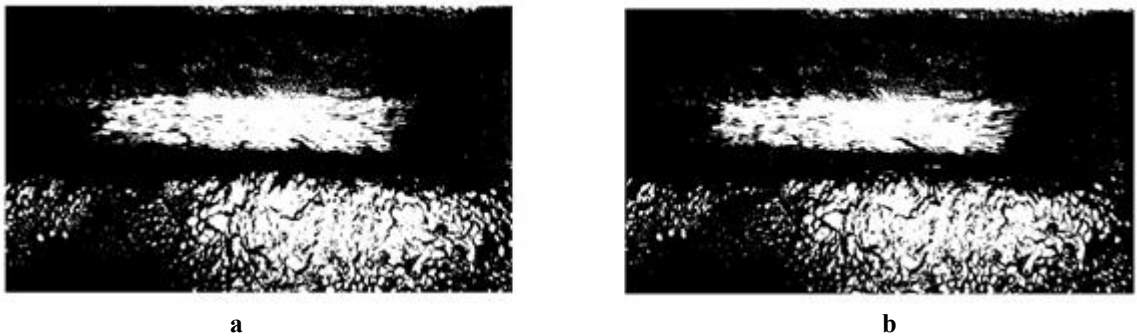
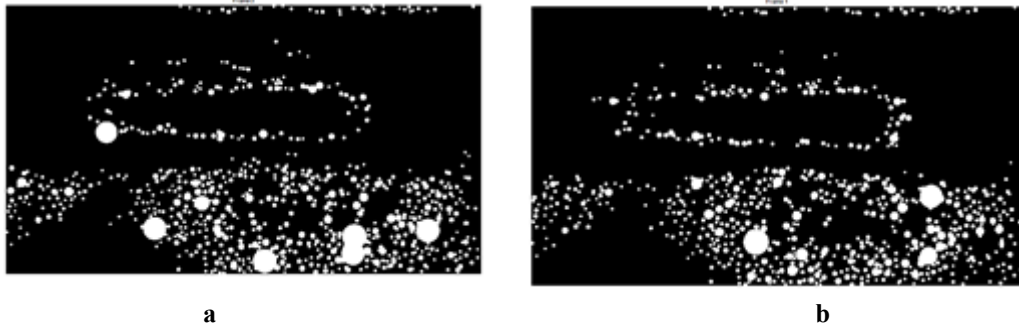


Fig. 3. a) Initial Frame b) Secondary Frame

In the second step, bubbles must be separated using the circular Hough transform algorithm. It should be noted that to increase the accuracy of bubble detection, reduce the effect of noise in the image, and increase the algorithm's resistance to various noises, a tuned edge detection algorithm is used. This helps in easily identifying sharp edges in the image. After finding the edges, for each circle in the input image, all points inside the circle are assumed to be the center of the circle. All these pixels are considered with coordinates  $(x_0, y_0)$  and all pixels on the edges with coordinates  $(x, y)$  are used to calculate the radius of the circle using the following relation:

$$r^2 = (x - x_0)^2 + (y - y_0)^2 \tag{4}$$

After calculating the radii for the pixels inside the circle, a three-dimensional matrix is initialized. The first and second dimensions store the coordinates of the circle's center, and the third-dimension stores different radii. The values in the matrix represent the number of pixels whose coordinates satisfy the equation above. If the number of these pixels on the circle's perimeter exceeds a threshold, it is recognized as a circle. The advantage of using the improved Hough transform is that it can identify bubbles with different radii. However, to determine the velocity, it is not necessary to identify all circles; rather, only those within a specific radius range can be extracted from the flotation froth images [15]. In other words, by increasing the parameters required to define the desired object, the dimensions of the parameter space increase, making the Hough transform more complex. To simplify the parameter space of the circle, the radius is recorded as a fixed number or within a specific range in this space. Applying the circular Hough transform to the frames is shown in Figure 4.



**Fig. 4.** a) Applying Hough Transform on Initial Frame b) Applying Hough Transform on Secondary Frame

The third step involves executing PIV on the two extracted frames. For image processing, two sequential images are compared, and bubble movement is observed. This involves tracking a bubble and observing its path change. For effective tracking, instead of tracking individual bubbles (PIV method), a group of bubbles is tracked to see where they move in the second image. For quantitative rather than qualitative analysis of the two images, they are converted into matrices of numbers where a higher number means more light. Then the main matrix is divided into smaller matrices, each representing a group of particles. These matrices are called scanning windows. The goal is to find a similar pattern in the second image. Quantitatively, a matrix that closely matches the first matrix is found in the second image. The similarity of the two matrices is defined as follows and is called correlation:

$$r = \frac{\sum_m \sum_n (A_{mn} - \bar{A})(B_{mn} - \bar{B})}{\sqrt{(\sum_m \sum_n (A_{mn} - \bar{A})^2)(\sum_m \sum_n (B_{mn} - \bar{B})^2)}} \tag{5}$$

Thus, the matrix in the second image with the highest correlation with the first scanning window is searched for. The distance between the centers of the two matrices indicates the displacement of the central point of the first matrix. There is no need to search the entire second image; only a larger matrix around the scanning window can be defined, and the search can be limited to that area [15]. The difference between the search matrix and the scanning window can be visually determined by observing sequential images and following bubble movement. The search matrix is considered sufficiently larger than the initial matrix. With the bubble displacement length and the time between the two frames, the bubble velocity in the image can be calculated. The displacement vector contour can be seen in Figure 5.

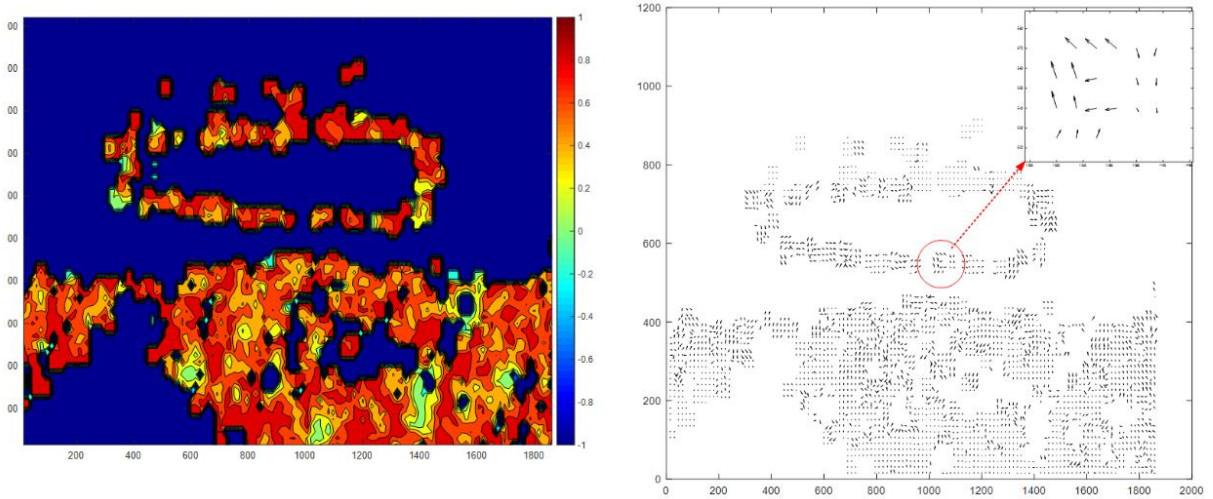


Fig. 5. Contour of Displacement Vectors in Two Frames from a Video

### 3. RESULTS

This study was conducted on the flotation process at the Miduk Copper Mine in Iran. This mine is located 42 kilometers northeast of Shahr-e Babak and 132 kilometers northwest of the Sarcheshmeh Copper Mine. The direct distance to Shahr-e Babak is 27 kilometers, and to Sarcheshmeh, it is 80 kilometers. To obtain the velocity vector quantity in standard measurement units, a calibrated image is required to serve as a measurement basis. For image registration, two points along the fluid flow path were considered, and their distance was measured. This distance, shown in Figure 6, is 48 centimeters. The number of pixels corresponding to this distance in the captured image is 1530 pixels. Additionally, the time interval between each captured image must be determined. The image capture speed of the camera is 30 frames per second. Considering that the fluid traveled 48 centimeters in approximately 39 frames, and given the camera's frame rate, the calculated speed is 0.39 meters per second. The speed calculation criterion based on pixel distance is shown in Figure 6.

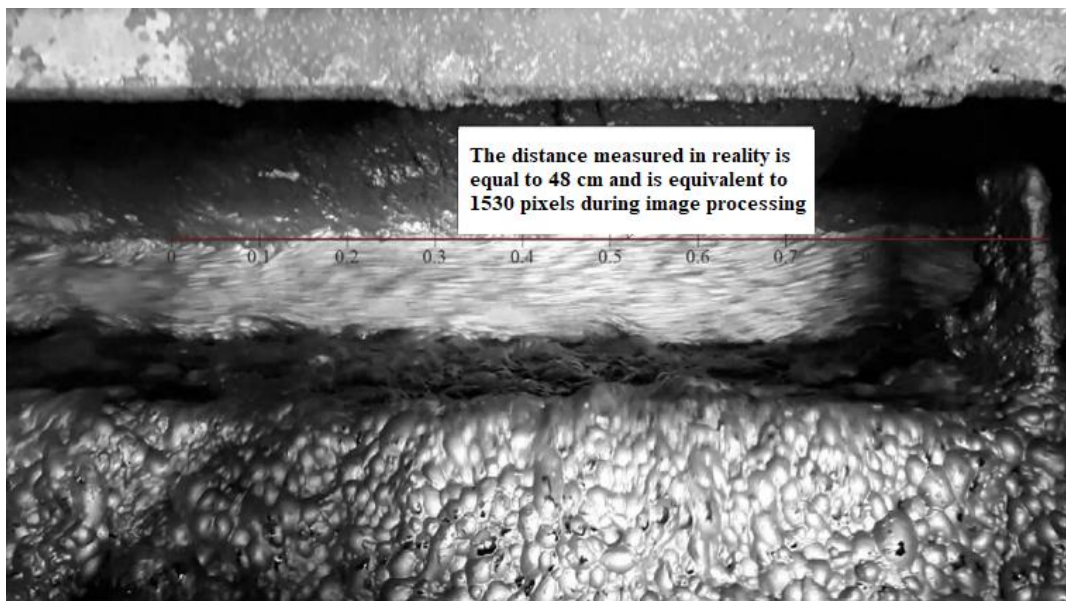


Fig. 6. Calibration of Measured Distance with Pixels in the Image

The characteristics obtained from the video images are shown in Table 1.

**Table 1.** Characteristics of Displacement Vectors and Speed in Flotation Video Images

Numbers of Two Frames	V(m/s)
15-16	0.35
20-21	0.33

Considering that the fluid moves in both horizontal and vertical directions and PIV calculations are applied to the entire image, the difference between the measured speed using image processing and the practical speed is logical.

#### 4. DISCUSSION

The PIV method has two major advantages. The first advantage is its non-interference with the flow, as all equipment used in this method is located outside the fluid. The second advantage is the ability to calculate the entire flow (a two-dimensional domain, i.e., a plane) at a moment. Additionally, if the camera's speed is high, fast phenomena in the fluid can be observed. One source of error in the PIV method is background light, which is why the experimental environment is darkened to only see the laser light. Since laser light is not used in the proposed method, this error will not occur. In modern technologies, implementing the PIV technique at high speeds requires a camera capable of capturing two consecutive frames and a pulsed laser. Given the low speed in flotation, standard industrial cameras can be used. The cameras used in the PIV technique must be digital to convert data into numbers. Also, the video captured by the camera should be frame-by-frame to obtain images at a specific and known time; otherwise, information read over time will not be useful. The noise in the camera includes the following: the first is reading error, which occurs mostly during data transfer, where electrons are added or subtracted from the data, resulting in errors in calculations. The second is dark noise, which relates to the heat in CCD cameras. Even if no light reaches the camera's CCD and the camera is ready for photography, electrons are released over time due to the surrounding heat, which leads to errors in the calculations. This noise occurs when the camera exposure time is very high, and cooling the camera can minimize this error. The third is shot noise, which relates to how light reaches the camera. If the light source is stable, the light reaching the camera is not continuous; for instance, 99 photons may reach the camera instead of 100, causing variability.

#### 5. CONCLUSION

In this study, a proposed method for monitoring the velocity of an industrial mechanical flotation cell was discussed. The froth velocity was extracted under different operating conditions. A simple and robust algorithm was developed to measure bubble velocity by tracking bubbles in sequential video images. The results showed that the extracted visual features could accurately describe process behavior under different operating conditions.

#### ACKNOWLEDGMENTS

I would like to extend my sincere gratitude to the National Iranian Copper Industries Company, especially the Shahr-e Babak Copper Complex, for their assistance in preparing this paper.

#### Transparency Statement

The data supporting this study are available upon reasonable request to the corresponding author, subject to ethical and confidentiality considerations.

## Declaration of Interest

The authors declare that they have no competing interests.

## Funding

This research received no specific grant from any funding agency, commercial, or not-for-profit sectors.

## REFERENCES

- [1] Velasco-Vélez, J., Jones, T., Gao, D., Carbonio, E., Arrigo, R., Hsu, C.-J., Huang, Y.-C., Dong, C., Chen, J.-M., Lee, J., Strasser, P., Cuenya, B. R., Schlögl, R., Knop-Gericke, A., & Chuang, C. (2018). The role of the copper oxidation state in the electrocatalytic reduction of CO<sub>2</sub> into valuable hydrocarbons. *ACS Sustainable Chemistry & Engineering*. <https://doi.org/10.1021/acssuschemeng.8b05106>
- [2] Jiang, Y., Fan, J., Chai, T., Li, J., & Lewis, F. (2018). Data-driven flotation industrial process operational optimal control based on reinforcement learning. *IEEE Transactions on Industrial Informatics*, 14, 1974-1989. <https://doi.org/10.1109/TII.2017.2761852>
- [3] Jabłońska, B., Kityk, A., Busch, M., & Huber, P. (2017). The structural and surface properties of natural and modified coal gangue. *Journal of Environmental Management*, 190, 80-90. <https://doi.org/10.1016/j.jenvman.2016.12.055>
- [4] Chen, X., & Peng, Y. (2018). Managing clay minerals in froth flotation—a critical review. *Mineral Processing and Extractive Metallurgy Review*, 39, 289-307. <https://doi.org/10.1080/08827508.2018.1433175>
- [5] Nakhaei, F., & Irannajad, M. (2018). Reagents types in flotation of iron oxide minerals: A review. *Mineral Processing and Extractive Metallurgy Review*, 39, 124-189. <https://doi.org/10.1080/08827508.2017.1391245>
- [6] Willis, B., & Napier-Munn, T. (2006). *Mineral processing technology: An introduction to the practical aspects of ore treatment and mineral recovery*. Elsevier Science & Technology Books.
- [7] Rao, S. R. (2013). *Surface chemistry of froth flotation: Volume 1: Fundamentals*. Springer Science & Business Media.
- [8] Zhang, X., Wang, H., He, L., Lu, K., Sarmah, A., & Li, J. (2013). Using biochar for remediation of soils contaminated with heavy metals and organic pollutants. *Environmental Science and Pollution Research*, 20(12), 8472-8483. <https://doi.org/10.1007/s11356-013-1659-0>
- [9] Mehrabi, A., Mehrshad, N., & Massinaei, M. (2014). Machine vision based monitoring of an industrial flotation cell in an iron flotation plant. *International Journal of Mineral Processing*, 133, 60-66. <https://doi.org/10.1016/j.minpro.2014.09.018>
- [10] Xu, D., Chen, X., Xie, Y., Yang, C., & Gui, W. (2015). Complex networks-based texture extraction and classification method for mineral flotation froth images. *Minerals Engineering*, 83, 105-116. <https://doi.org/10.1016/j.mineng.2015.08.017>
- [11] Moolman, D., Aldrich, C., Schmitz, G., & Van Deventer, J. (1996). The interrelationship between surface froth characteristics and industrial flotation performance. *Minerals Engineering*, 9(8), 837-854. [https://doi.org/10.1016/0892-6875\(96\)00076-3](https://doi.org/10.1016/0892-6875(96)00076-3)

- [12] Wang, W., Bergholm, F., & Yang, B. (2003). Froth delineation based on image classification. *Minerals Engineering*, 16(11), 1183-1192. <https://doi.org/10.1016/j.mineng.2003.07.014>
- [13] Raffel, M., Willert, C. E., Scarano, F., Kähler, C. J., Wereley, S. T., & Kompenhans, J. (2018). *Particle image velocimetry: A practical guide*. Springer. <https://doi.org/10.1007/978-3-319-68852-7>
- [14] Brownlee, C., Pegoraro, V., Shankar, S., McCormick, P., & Hansen, C. D. (2011). Physically-based interactive flow visualization based on schlieren and interferometry experimental techniques. *IEEE Transactions on Visualization and Computer Graphics*, 17(11), 1574-1586. <https://doi.org/10.1109/TVCG.2010.255>
- [15] Ansari, A. (2016). Parametric study of free convective flow and heat transfer around a horizontal heated circular cylinder inside a vertical channel using PIV technique (M.Sc. thesis, Isfahan University of Technology, Isfahan, Iran).